Research Article

Journal of PeptideScience

Received: 3 July 2008 Revised: 26 September 2008 Accepted: 26 September 2008 Published online in Wiley Interscience: 26 November 2008

(www.interscience.com) DOI 10.1002/psc.1086

A thermodynamic approach to the conformational preferences of the 180–195 segment derived from the human prion protein α2-helix‡

Luisa Ronga, Pasquale Palladino, Raffaele Ragone, Ettore Benedetti and Filomena Rossi*

On consideration that intrinsic structural weakness could affect the segment spanning the α2-helical residues 173–195 of the PrP, we have investigated the conformational stabilities of some synthetic Ala-scanned analogs of the peptide derived from the 180–195 *C*-terminal sequence, using a novel approach whose theoretical basis originates from protein thermodynamics. Even though a quantitative comparison among peptides could not be assessed to rank them according to the effect caused by single amino acid substitution, as a general trend, all peptides invariably showed an appreciable preference for an α-type organization, consistently with the fact that the wild-type sequence is organized as an α-helix in the native protein. Moreover, the substitution of whatever single amino acid in the wild-type sequence reduced the gap between the α- and the β-propensity, invariably enhancing the latter, but in any case this gap was larger than that evaluated for the full-length α2-helix-derived peptide. It appears that the low β-conformation propensity of the 180–195 region depends on the simultaneous presence of all of the Ala-scanned residues, indirectly confirming that the *N*-terminal 173–179 segment could play a major role in determining the chameleon conformational behavior of the entire 173–195 region in the PrP.

Keywords: prion protein; α2-helix; β-sheet; amyloid; transmissible spongiform encephalopathies; CD titration; prion toxicity; structure-inducing agents

Introduction

Prion diseases are a group of transmissible neurodegenerative disorders that enclose scrapie in sheep, bovine spongiform encephalopathy (BSE), and Creutzfeldt–Jakob disease (CJD), fatal insomnia and Gerstmann–Sträussler–Scheinker disease in humans. The pathogenic mechanism underlying these diseases is a conformational conversion of the PrP^{C} into disease-specific species (PrP^{Sc}) that possess abnormal physicochemical properties, such as insolubility and protease resistance, and accumulate in the brain in the form of amorphous aggregates and amyloid fibrils [1]. Despite a large number of studies, possible causes of PrP^{C} pathogenic conversion and its role in cellular function still remain unclear. Moreover, the highly aggregated state of the abnormal form has hampered the elucidation of the PrP^{Sc} structure at the atomic level.

The importance of PrP studies has remarkably increased following the BSE epidemic and the appearance of a new variant of CJD that seems to be causally linked to it [2–4]. Moreover, given that general features of prion diseases are common to other amyloid disorders [5], the PrP could be used as a model to provide the bases for a comprehensive evaluation of the general protein misfolding mechanism. It is therefore evident that a conformation-based approach to the study of PrP can give useful hints both on the region/residues potentially important for the $PrP^{C} \rightarrow PrP^{Sc}$ conversion and on the identification or development of antiprion compounds.

We have been interested in a peptide (PrP [173–195]) corresponding to the α2-helix of human PrP^{C} [6], which possesses chameleon conformational behavior, gathers several disease-promoting point mutations, and can be strongly fibrillogenic and toxic to neuronal cells [7]. Studies on the conformational properties of this fragment [6,8], on its affinity toward potential PrP-binding compounds [9], and on other synthetic α2-helix-derived peptides suggest that the α2-helical region is involved in prion aggregation and toxicity associated to the scrapie isoform, providing support to recently reported evidence [10]. In particular, CD and NMR investigations point to ascribe predicted low α-helical content and high β-sheet propensity, as well as conformational weakness of the full 173–195 sequence to the 180–195 fragment [6,11], which could be involved in the nucleation process of prion misfolding and oligomerization [12]. The corresponding peptide (PrP [180–195]) includes the highly conserved threonine-rich 188–195

* *Correspondence to: Filomena Rossi, Dipartimento delle Scienze Biologiche and C.I.R.Pe.B., Università Federico II di Napoli, Via Mezzocannone 16, Naples 80134, Italy. E-mail: filomena.rossi@unina.it*

Dipartimento delle Scienze Biologiche and C.I.R.Pe.B., Università Federico II di Napoli, Naples, Italy

Abbrevations used: *PrP, prion protein; PrP^{C}, cellular PrP; PrP^{Sc}, scrapie PrP; SDS, sodium dodecyl sulfate; TFE, 2,2,2-trifluoroethanol.*

‡ *Dedicated to Prof. Carlo Pedone on the occasion of his 70th birthday.*

Journal of PeptideScience

C-terminal part of the PrP^C full-length helix 2 and is devoid of effects linked to the reactivity of the thiolic cysteine side chain. The organization of PrP [180–195] has already been shown to be affected by buffer composition via the ion charge density dependence typical of Hofmeister effects [13], and may even be induced into a β-type conformation that only very high amounts of TFE are able to modify into a fully helical conformation, in spite of the fact that the parent sequence is fully helical in the native protein [11].

In the present study, we analyze the α- and β-propensities of a series of Ala-scanned analogs of the PrP [180–195] peptide, as evaluated by the thermodynamic tendencies to acquire secondary structure in structure-inducing media, namely TFE and submicellar SDS, respectively, at neutral pH and room temperature. The Ala-scanned region was chosen starting from His187, according to previously reported evidence that the full PrP α2-helix possesses a locus of intrinsic structural weakness centered on Lys185 and Gln186 [8,11]. Our original purpose was to compare the effect of single amino acid substitutions on driving the peptide arrangement, quantitatively ranking the peptides according to their α- and β-propensities. Results were quite difficult to analyze in this context. However, as a common trend, different amino acid replacements invariably enhanced the propensity to assume a β-conformation, making any Ala-scanned peptide more prone to structural rearrangements than the wild-type peptide. Overall, it appears that all of the Ala-scanned residues substantially favor the α-helical organization of the full 173–195 region in the PrP and that the N-terminal 173–179 segment could play a major role in the delicate balance of forces that control the chameleon conformational behavior of this region.

Materials and Methods

Chemicals

HPLC chemicals were purchased from Lab-Scan (Dublin, Ireland), and the remainder of organic reagents were from Sigma-Aldrich (Milan, Italy). All solvents were reagent grade. *N*-α-Fmoc-protected amino acids and activating agents were purchased from Inbios (Pozzuoli, Italy). Resin for peptide synthesis was from Novabiochem (Läufelfingen, Switzerland). Columns for peptide purification and characterization were from Phenomenex (Torrance, CA, USA). SDS and TFE were obtained from Sigma-Aldrich (Milano, Italia) and Romil LTD (Dublin, Ireland), respectively.

Peptide Synthesis and Characterization

The *N*- and *C*-blocked peptides listed in Table 1 were synthesized in batch by standard 9-fluorenylmethyl carbamate chemistry protocol on Rink-amide 4-methylbenzhydrylamine (MBHA) resins. After peptide assembling, acetylation was carried out by 1 M acetic anhydride in dimethylformamide containing 5% *N*,*N*-diisopropyl ethylamine. Cleavage from the solid support was achieved by treatment with trifluoroacetic acid/triisopropylsilane/water (TFA/TIS/H_2O, 90 : 5 : 5 v/v/v) mixture for 90 min at room temperature. Then, peptides were precipitated in ether, dissolved in water/acetonitrile (1 : 1 v/v) mixture, lyophilized and purified by RP-HPLC using a C_{18} Jupiter (250 × 22 mm^2) column with a 10–60% linear gradient of acetonitrile in 0.1% TFA over 50 min. Peptide purity and integrity were confirmed by RP-HPLC analysis and liquid chromatography–mass spectrometry (Finnigan Surveyor, Thermo Electron Corporation).

Table 1. Peptides used in the present study

Abbreviation	Sequence
PrP [180–195] (wt)	Ac-V-N-I-T-I-K-Q-H-T-V-T-T-T-T-K-G-NH_2
PrP [180–195] H187A	Ac-V-N-I-T-I-K-Q-**A**-T-V-T-T-T-T-K-G-NH_2
PrP [180–195] T188A	Ac-V-N-I-T-I-K-Q-H-**A**-V-T-T-T-T-K-G-NH_2
PrP [180–195] V189A	Ac-V-N-I-T-I-K-Q-H-T-**A**-T-T-T-T-K-G-NH_2
PrP [180–195] T190A	Ac-V-N-I-T-I-K-Q-H-T-V-**A**-T-T-T-K-G-NH_2
PrP [180–195] T192A	Ac-V-N-I-T-I-K-Q-H-T-V-T-T-**A**-T-K-G-NH_2
PrP [180–195] T193A	Ac-V-N-I-T-I-K-Q-H-T-V-T-T-T-**A**-K-G-NH_2
PrP [180–195] K194A	Ac-V-N-I-T-I-K-Q-H-T-V-T-T-T-T-**A**-G-NH_2

Circular Dichroism

TFE and submicellar SDS titrations were based on the notion that peptides may be induced into α- or β-structure in these media [14–16]. The working concentration of SDS was chosen on the basis of its critical micelle concentration (CMC) at room temperature (4 mM) [17–19]. All peptides were dissolved in 10 mM phosphate buffer, pH 7.2, at 20 μM concentration, as obtained by dry weight. Then, TFE and SDS titration experiments were carried out using 10-mm quartz cells on a Jasco J-715 spectropolarimeter equipped with a thermostated water bath. Then, for each concentration of structuring agent, far UV CD spectra were recorded from 190 to 260 nm at room temperature (295 K). Each spectrum was obtained averaging three scans, subtracting the blank, and converting the signal to mean residue ellipticity in units of $degcm^2\ d\ mol^{-1}\ res^{-1}$. Other experimental settings were: 20 nm min^{-1}, scan speed; 2.0 nm, band width; 0.2 nm, resolution; 50 mdeg, sensitivity and 4 s, response.

Treatment of Data

For either TFE or SDS titrations, we assumed a two-state model and evaluated free energy changes for the transition induced by changing the solvent medium from the aqueous buffer to a structure-inducing condition, extrapolating isothermal titration data to zero concentration of added substance. Pertinent equations were implemented in the general-purpose nonlinear fitting program Scientist from MicroMath Software (San Diego, CA, USA), as described below.

For TFE, the ellipticity at a convenient wavelength (Θ_λ) was analyzed using a six-parameter model analogous to that previously derived for absorption [20] or fluorescence denaturation [21], which assumes a linear dependence of pre- and posttransition baselines on the TFE concentration, according to the function:

$$\Theta_\lambda = \frac{\Theta_r^\circ + m_r C + (\Theta_\alpha^\circ + m_\alpha C)\exp[-(\Delta G_\alpha^\circ + mC)/(RT)]}{\{1 + \exp[-(\Delta G_\alpha^\circ + mC)/(RT)]\}} \quad (1)$$

Here, the TFE concentration is given by *C*, the pretransition dichroic signal intercept (0% TFE) and slope are Θ_r° and m_r, respectively, the helical state dichroic signal intercept and slope are Θ_α° and m_α, respectively, the secondary structure formation free energy function intercept and slope are ΔG_α° and *m*, respectively, *R* is the universal gas constant, and *T* represents the absolute temperature. For fitting purposes, it was decided by visual inspection whether and which of the slopes of pre- and posttransition baselines were to be used as fitting parameters, otherwise they were set to zero.

For SDS, the dichroic signal was analyzed using a function analogous to that adopted for TFE, expressing the dependence of the free energy on the detergent concentration by a binding isotherm, according to the seven-parameter equation:

$$\Theta_\lambda = \frac{\{\Theta_r^\circ + m_r D + (\Theta_\beta^\circ + m_\beta D)\exp[-\Delta G_\beta^\circ/(RT) + \ln(1+kD)^{\Delta n}]\}}{\{1+\exp[-\Delta G_\beta^\circ/(RT) + \ln(1+kD)^{\Delta n}]\}} \quad (2)$$

Here, the SDS concentration is given by D, the pretransition dichroic signal intercept (0% SDS) and slope are Θ_r° and m_r, respectively, and the β-state dichroic signal intercept and slope are Θ_β° and m_β, respectively. The free energy of secondary structure formation in the absence of SDS is given by ΔG_β°, and Δn represents the excess of the peptide detergent binding sites in the β-state characterized by the intrinsic binding constant k. Owing to the strong correlation between k and Δn, curve fitting was carried out using $k = 50\,000\ \text{M}^{-1}$, which is the value found for SDS interaction with electrostatic binding sites of small proteins [22]. This model has already been shown to work for micellar aggregation [23] and is under further development in our laboratory (Ragone *et al.*, unpublished observation). Fitting procedures were the same as those described above for TFE.

Results and Discussion

The first set of experiments was carried out monitoring TFE-induced modifications of the far UV CD spectrum of peptides at room temperature. TFE is a hydrophilic and hydrogen-bonding solvent that belongs to a group of organic substances such as methanol, ethanol, acetonitrile, 1,1,1,3,3,3-hexafluoroisopropanol at low pH, octanol mixed with other alcoholic solvents and SDS at high concentrations, which are known to induce secondary structure in peptides [24–26]. In fact, it is well known that TFE–water mixtures increase the population of α-helix and β-sheet content in secondary-structure-forming peptides [27–30]. We have also reported [8] that TFE may be used to mimic a native-like environment for peptide fragments whose conformation in solution is different from that observed in the parent protein.

Above about 40% TFE, the spectra of all peptides were those typical of helical structure, with pronounced minima at 208 and 222 nm and a strong positive maximum at 191–193 nm [31], suggesting an intrinsic preference for α-helix formation. This structural modification was in any case reversible. Thus, dichroic activity data as a function of the TFE concentration were best fitted to Eqn (1), assuming two-state behavior and a linear dependence of the free energy of helix formation on the concentration of TFE, i.e. $\Delta G_{TFE}^\circ = \Delta G_\alpha^\circ + mC$. This procedure is similar to the linear extrapolation of the unfolding free energy of globular proteins to zero denaturant concentration, as previously reported [28–30]. The free energy (ΔG_α°) in the absence of structuring agent was then obtained as a fitting parameter. As an example, Figure 1 shows CD spectra and curve fitting for PrP [180–195] T190A, as obtained in buffer solution after addition of TFE up to 50% (13.9 mol kg^{-1}).

A second set of experiments was carried out using SDS as the structuring agent, based on the notion that peptides may be induced into a β-sheet structure at submicellar concentrations of this substance [14–16]. There is a large body of literature about the nature of this solvent system, which has been described as a mimetic of protein interiors. It is commonly accepted that the nonpolar tails provide a template for the hydrophobic domains of peptides, mimicking the environment found in the interior of the parent protein, whereas the sulfate moiety helps solvation of the β-structured peptide. For all peptides, the addition of SDS reversibly resulted in spectra with positive and negative bands near 195–200 and 216–220 nm, respectively, which can be ascribed to a β-type profile [31]. Then, for each peptide, dichroic activity data were best fitted to Eqn (2) to obtain the transition free energy (ΔG_β°) in the absence of SDS, which was evaluated as a fitting parameter.

The binding isotherm that describes the dependence of the free energy on the surfactant concentration, i.e. $\Delta G_{SDS}^\circ = \Delta G_\beta^\circ + RT\ln(1+kD)^{\Delta n}$, is analogous to the model used for denaturation curves of proteins, better known as the denaturant binding model [32, 33]. This model leads to thermodynamic inconsistencies with protein denaturation, where very weak binding occurs, but is accurate in the present case, where few positively charged residues can act as distinct independent binding sites of high strength that assist the conversion of the

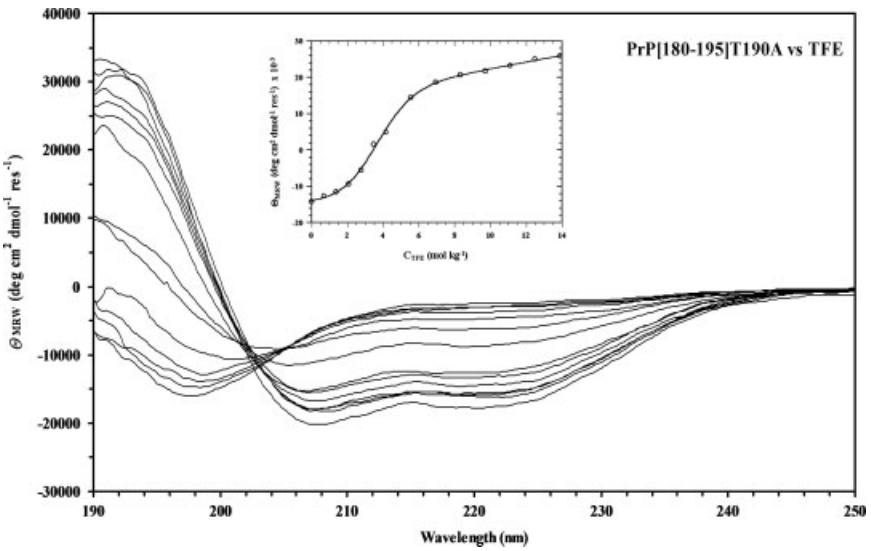

Figure 1. Far UV CD spectra of PrP [180–195] T190A in the presence of TFE. Increasing amounts of TFE (0–50%, v/v) were added to 20-μM peptide dissolved in buffer solution at pH 7. The inset shows best fitting of ellipticity at 195 nm versus TFE concentration (mol kg^{-1}) data to Eqn (1), as described in the text.

peptide from the unbound- to the SDS-bound form [34]. Formally, the binding of ionic surfactant to water-soluble proteins occurs through electrostatic (higher affinity) and nonpolar (lower affinity) binding sites. It is therefore conceivable that the driving force for peptide organization at low SDS concentration could be the presence of exposed cationic binding sites. Indeed, the fitting procedure resulted in $1.4 < \Delta n < 2.7$ for all peptides examined, which is in good agreement with the number of positively charged side chains in the peptide (two lysines and one histidine in PrP [180–195]). As an example, Figure 2 shows CD spectra and curve fitting for PrP [180–195] T190A, as obtained in buffer solution after addition of SDS up to 4 mM.

Table 2 summarizes free energy values obtained as described above. It would be desirable to use these data to rank the peptides according to their $\Delta G^{\circ}_{\alpha}$ and ΔG°_{β} values, as a measure of the effect produced by a single amino acid substitution on the propensity for a specific secondary structure. Indeed, this would be feasible if the pretransition structural state were the same for all peptides. Unfortunately, this was not the case, as could be judged on the basis of CD spectra (not shown), which were not always those typical of random organization. This shortcoming, however, does not interfere with the fact that all peptides can be compared on the basis of the free energy change required for the conversion from the α- to the β-conformation, as evaluated by $\Delta G^{\circ}_{\beta} - \Delta G^{\circ}_{\alpha}$ values, which are not affected by the pretransition structural state.

As shown in the fourth column of Table 2, $\Delta G^{\circ}_{\beta} - \Delta G^{\circ}_{\alpha}$ values are all positive, as all $\Delta G^{\circ}_{\alpha}$ values are lower than the corresponding ΔG°_{β} values, indicating that the conversion between the two forms is shifted toward the α-conformation for all peptides. This also occurs for the wild-type (wt) peptide (PrP [180–195]), in spite of the fact that its predominant conformation at neutral pH is β-type [11]. Indeed, the wild-type sequence is organized as an α-helix in the native protein. This systematic behavior is consistent with the intrinsic preference for α-helix formation in water–TFE mixtures, but is at odds with secondary structure predictions, which favor the β-conformation because of the elevated number of threonine residues. We do not presently have any explanation for such a behavior, but the fact that the peptide fragment approach is

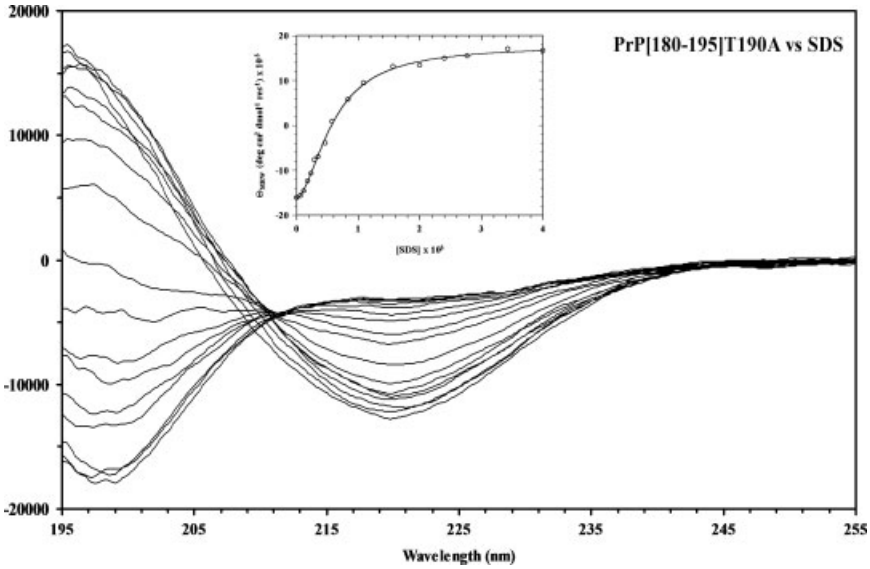

Figure 2. Far UV CD spectra of PrP [180–195] T190A in the presence of submicellar SDS. Increasing amounts of SDS (0–4 mM) were added from a concentrated stock solution to 20 μM peptide dissolved in buffer solution at pH 7. The inset shows best fitting of ellipticity at 195 nm *versus* SDS concentration data to Eqn (2), as described in the text. The SDS concentration was expressed in molar units, consistently with the units of the intrinsic binding constant (50 000 M^{-1}, See Section on Materials and Methods for details). This does not produce any substantial difference in the fitting values, because here the difference between molar and molal units is negligibly small due to the low SDS concentration.

Table 2. Thermodynamic stabilities of peptides[a]

Peptide	$\Delta G^{\circ}_{\alpha}$	ΔG°_{β}	$\Delta G^{\circ}_{\beta} - \Delta G^{\circ}_{\alpha}$	$\Delta G^{\circ}_{\alpha} - \Delta G^{\circ}_{\alpha,wt}$	$\Delta G^{\circ}_{\beta} - \Delta G^{\circ}_{\beta,wt}$
PrP [180–195] (wt)	8.4 ± 2.8	27.1 ± 4.2	18.7 ± 7.0	0	0
PrP [180–195] H187A	7.9 ± 3.2	ND	ND	−0.5 ± 6.0	ND
PrP [180–195] T188A	9.7 ± 3.7	15.0 ± 3.0	5.3 ± 6.7	1.3 ± 6.5	−12.1 ± 7.2
PrP [180–195] V189A	4.9 ± 1.3	15.0 ± 1.6	10.1 ± 2.9	−3.5 ± 4.1	−12.1 ± 5.8
PrP [180–195] T190A	8.7 ± 2.1	15.3 ± 0.8	6.6 ± 2.9	0.3 ± 4.9	−11.8 ± 5.0
PrP [180–195] T192A	7.1 ± 2.8	20.1 ± 3.4	13.0 ± 6.2	−1.3 ± 5.6	−7.0 ± 7.6
PrP [180–195] T193A	8.5 ± 2.4	15.0 ± 1.0	6.5 ± 3.4	0.1 ± 5.2	−12.1 ± 5.2
PrP [180–195] K194A	7.3 ± 1.3	19.5 ± 2.2	12.2 ± 3.5	−1.1 ± 4.1	−7.6 ± 6.4

ND, not determined.
The errors on $\Delta G^{\circ}_{\alpha}$ and ΔG°_{β} are standard deviations obtained by the fitting procedure. The errors on the remaining figures were calculated by propagation.
[a] All values are in kJ mol^{-1}.

rather rough to take thoroughly into account intrinsic and extrinsic structural constraints that are effective in the native protein. A further possibility is that the accurate evaluation of amino acid conformational preferences in the presence of consecutive homo-residues requires further investigation.

It can be also appreciated that all substitutions produce lower $\Delta G^{\circ}_{\beta} - \Delta G^{\circ}_{\alpha}$ values as compared to the wild-type peptide, indicating an increased tendency of substituted peptides to acquire a β-type conformation. The last two columns of Table 2 show that increments in secondary structure stability ($\Delta\Delta G^{\circ}$) caused by single amino acid substitution in the wild-type PrP [180–195] peptide are in any case negative and much larger for β-structure ($\Delta\Delta G^{\circ}_{\beta} = \Delta G^{\circ}_{\beta} - \Delta G^{\circ}_{\beta,\mathrm{wt}}$) compared to α-helix ($\Delta\Delta G^{\circ}_{\alpha} = \Delta G^{\circ}_{\alpha} - \Delta G^{\circ}_{\alpha,\mathrm{wt}}$). This confirms that any single residue substitution with Ala invariably renders the fragment more prone to a conformationally ambiguous behavior, increasing the peptide tendency to assume a β-type organization through small alterations of $\Delta\Delta G^{\circ}_{\alpha}$, i.e. only marginally altering the α-propensity, but appreciably larger $\Delta\Delta G^{\circ}_{\beta}$ values. In order to find a possible explanation of how this may occur, it is useful to inspect the NMR structure of PrP [180–195] in a native-like environment, as mimicked by neat TFE (pdb code: 2iv4) [11]. Indeed, all Ala-scanned residues, which, as stated above, lie immediately after the locus of intrinsic structural weakness centered on Lys185 and Gln186 [8,11], are located in an extended region stabilized by H-bonds between threonine side chains and peptide backbone, in which: (i) any Thr-to-Ala replacement causes reduction of H-bonds; (ii) the Val-to-Ala substitution leads to decreased steric hindrance and (iii) the Lys-to-Ala mutation removes the Lys–Lys repulsion. Any of these circumstances may favor backbone–backbone interaction between *N*- and *C*-termini, thus facilitating a β-hairpin conformation (Figure 3). Furthermore, it is also worth stressing that the $\Delta G^{\circ}_{\beta} - \Delta G^{\circ}_{\alpha}$ value typical of each peptide is generally larger than that evaluated for the full-length α2-helix-derived peptide (PrP [173–195]), which has been previously shown to amount to about 5 kJ mol^{-1} at room temperature [6]. This suggests that the *N*-terminal 173–179 segment could play a major role in determining the conformational ambiguity of the entire α2-helix, confirming recently reported evidence that it controls the structural organization of the *C*-terminal 180–195 region [11].

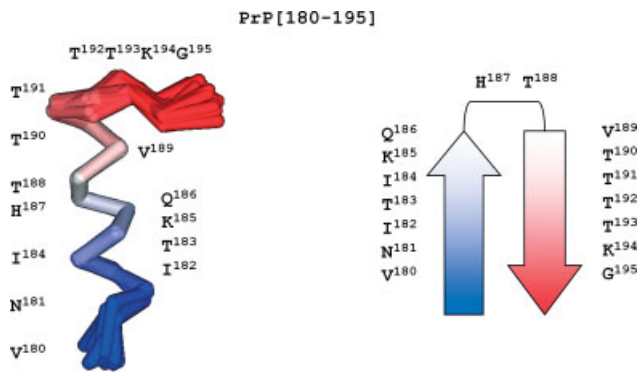

Figure 3. Scheme of PrP [180–195] conformations. The left panel shows the NMR structure in neat TFE (pdb code: 2iv4), in which the extended *C*-terminal region is stabilized by H-bonds between threonine side chains and peptide backbone. The right panel depicts a hypothetical β-hairpin conformation, in which the first two residues of the Ala-scanned region (His187 and Thr188), lying immediately after the locus of intrinsic structural weakness centered on Lys185 and Gln186 [8,11], represent the *C*- and *N*-terminus of the first and the second antiparallel strands, respectively.

Conclusions

Recent studies point to ascribe the conformational weakness of the full 173–195 sequence to the 180–195 fragment, whose Thr-rich sequence is expected to favor low α-helical content and high β-sheet propensity, thus being putatively involved in the conversion of PrP^{C} into fibrillar PrP^{Sc}. Indeed, the $\alpha \rightarrow \beta$ isomerization of PrP most frequently observed *in vitro* in the pH range from 4 to 7 [35–39], and postulated to be induced *in vivo* by the low pH of endosomal compartments [40], has been suggested to be driven by one of the two potential loci of β-structure propagation (residues 188–204) identified in the X-ray structure of monomeric sheep PrP^{C} ($sPrP^{C}$) [12], acting as an $\alpha \rightarrow \beta$ switch within the monomeric protein. In addition, a comparison between the C-terminus crystal structures of monomeric sheep and dimeric human PrP^{C}s shows that the dimer results from the swapping of the C-terminal α-helix 3 and rearrangement of the Cys179–Cys214 disulfide bond. As a result, the corresponding crystal-symmetry-related residues 190–194, which are located in α-helix 2 in the monomeric NMR structures [41], form an interchain two-stranded antiparallel β-sheet at the dimer interface. Finally, the segment 188–201 (TVTTTTKGENFTET) is invariant across a wide variety of species [42], even adopting an architecture that appears to be of lower stability as compared to the rest of the human PrP structure, and lies immediately after Lys185 and Gln186, a locus to which intrinsic structural weakness has been attributed. Therefore, it has been suggested that the seven threonine residues could confer the conformational plasticity necessary for driving PrP^{C} reorganization.

According to the peptide fragment assumption, the present work aims at providing a thermodynamic basis to structural investigations on the relative stability of the α2-helical 180–195 segment of the PrP. Using a theoretical approach that is based on well-known methods of protein thermodynamics, and TFE and submicellar SDS as α- and β-structure inducers, respectively, we have investigated the conformational propensities of Ala-scanned analogs of the wild-type PrP [180–195] peptide. Extrapolation of free energy data to zero concentration of structuring agent highlighted that all peptides have in common a substantial preference for an α-helical organization, in spite of their expected high β-propensity. Several single amino acid substitutions systematically draw the stability of the β-conformation closer to that of the α-helix, suggesting that the low β-conformation propensity of the 180–195 region does not depend on the presence of any specific Ala-scanned residue. This indirectly confirms that the *N*-terminal 173–179 segment could play a major role in determining the ambiguous conformational behavior of the entire 173–195 region in the PrP.

Acknowledgements

The authors acknowledge the Internazionalizzazione del Sistema Universitario 2004-2006, MIUR D.M. 5.8.2004 n. 262, art. 23, for its support to this research.

References

1. Prusiner SB. Prions. *Proc. Natl. Acad. Sci. U.S.A.* 1998; **95**: 13363–13383.
2. Will RG, Ironside JW, Zeidler M, Cousens SN, Estibeiro K, Alperovitch A, Poser S, Pocchiari M, Hofman A, Smith PG. A new variant of Creutzfeldt-Jakob disease in the UK. *Lancet* 1996; **347**: 921–925.

3. Collinge J, Sidle KC, Meads J, Ironside J, Hill AF. Molecular analysis of prion strain variation and the aetiology of 'new variant' CJD. *Nature* 1996; **383**: 685–690.
4. Bruce ME, Will RG, Ironside JW, McConnell I, Drummond D, Suttie A, McCardle L, Chree A, Hope J, Birkett C, Cousens S, Fraser H, Bostock CJ. Transmissions to mice indicate that 'new variant' CJD is caused by the BSE agent. *Nature* 1997; **389**: 498–501.
5. Temussi PA, Masino L, Pastore A. From Alzheimer to Huntington: why is a structural understanding so difficult? *EMBO J.* 2003; **22**: 355–361.
6. Tizzano B, Palladino P, De Capua A, Marasco D, Rossi F, Benedetti E, Pedone C, Ragone R, Ruvo M. The human prion protein alpha2 helix: a thermodynamic study of its conformational preferences. *Proteins* 2005; **59**: 72–79.
7. Thompson A, White AR, McLean C, Masters CL, Cappai R, Barrow CJ. Amyloidogenicity and neurotoxicity of peptides corresponding to the helical regions of PrP(C). *J. Neurosci. Res.* 2000; **62**: 293–301.
8. Ronga L, Palladino P, Saviano G, Tancredi T, Benedetti E, Ragone R, Rossi F. NMR structure and CD titration with metal cations of human prion alpha2-helix-related peptides. *Bioinorg. Chem. Appl.* 2007; 10720.
9. Ronga L, Langella E, Palladino P, Marasco D, Tizzano B, Saviano M, Pedone C, Improta R, Ruvo M. Does tetracycline bind helix 2 of prion? An integrated spectroscopical and computational study of the interaction between the antibiotic and alpha helix 2 human prion protein fragments. *Proteins* 2007; **66**: 707–715.
10. Lu X, Wintrode PL, Surewicz WK. Beta-sheet core of human prion protein amyloid fibrils as determined by hydrogen/deuterium exchange. *Proc. Natl. Acad. Sci. U.S.A.* 2007; **104**: 1510–1515.
11. Ronga L, Palladino P, Saviano G, Tancredi T, Benedetti E, Ragone R, Rossi F. Structural characterization of a neurotoxic threonine-rich peptide corresponding to the human prion protein α-2 helical 180–195 segment, and comparison with full length α2-helix-derived peptides. *J. Pept. Sci.* 2008; **14**: 1096–1102.
12. Haire LF, Whyte SM, Vasisht N, Gill AC, Verma C, Dodson EJ, Dodson GG, Bayley PM. The crystal structure of the globular domain of sheep prion protein. *J. Mol. Biol.* 2004; **336**: 1175–1183.
13. Ronga L, Palladino P, Tizzano B, Marasco D, Benedetti E, Ragone R, Rossi F. Effect of salts on the structural behaviour of hPrP alpha2-helix-derived analogues: the counterion perspective. *J. Pept. Sci.* 2006; **12**: 790–795.
14. Zhong L, Johnson WC Jr. Environment affects amino acid preference for secondary structure. *Proc. Natl. Acad. Sci. U.S.A.* 1992; **89**: 4462–4465.
15. Wu CS, Yang JT. Sequence-dependent conformations of short polypeptides in a hydrophobic environment. *Mol. Cell. Biochem.* 1981; **40**: 109–122.
16. Wu CS, Ikeda K, Yang JT. Ordered conformation of polypeptides and proteins in acidic dodecyl sulfate solution. *Biochemistry* 1981; **20**: 566–570.
17. Esposito C, Colicchio P, Facchiano A, Ragone R. Effect of a weak electrolyte on the critical micellar concentration of sodium dodecyl sulfate. *J. Colloid Interface Sci.* 1998; **200**: 310–312.
18. Le Maire M, Champeil P, Møller JV. Interaction of membrane proteins and lipids with solubilizing detergents. *Biochim. Biophys. Acta* 2000; **1508**: 86–111.
19. Kuroda Y, Maeda Y, Sawa S, Shibata K, Miyamoto K, Nakagawa T. Effects of detergents on the secondary structures of prion protein peptides as studied by CD spectroscopy. *J. Pept. Sci.* 2003; **9**: 212–220.
20. Santoro MM, Bolen DW. Unfolding free energy changes determined by the linear extrapolation method. 1. Unfolding of phenylmethanesulfonyl alpha-chymotrypsin using different denaturants. *Biochemistry* 1988; **27**: 8063–8068.
21. Eftink MR. The use of fluorescence methods to monitor unfolding transitions in proteins. *Biophys. J.* 1994; **66**: 482–501.
22. Bordbar AK, Saboury AA, Housaindokht MR, Moosavi-Movahedi AA. Statistical effects of the binding of ionic surfactant to protein. *J. Colloid Interface Sci.* 1997; **192**: 415–419.
23. Ambrosone L, Ragone R. The interaction of micelles with added species and its similarity to the denaturant binding model of proteins. *J. Colloid Interface Sci.* 1998; **205**: 454–458.
24. Nelson JW, Kallenbach NR. Stabilization of the ribonuclease S-peptide α-helix by trifluoroethanol. *Proteins* 1986; **1**: 211–217.
25. Nelson JW, Kallenbach NR. Persistence of the alpha-helix stop signal in the S-peptide in trifluoroethanol solutions. *Biochemistry* 1989; **28**: 5256–5261.
26. Merutka G, Stellwagen E. Analysis of peptides for helical prediction. *Biochemistry* 1989; **28**: 352–357.
27. Roccatano D, Colombo G, Fioroni M, Mark AE. Mechanism by which 2,2,2-trifluoroethanol/water mixtures stabilize secondary-structure formation in peptides: a molecular dynamics study. *Proc. Natl. Acad. Sci. U.S.A.* 2002; **99**: 12179–12184.
28. Jasanoff A, Fersht AR. Quantitative determination of helical propensities from trifluoroethanol titration curves. *Biochemistry* 1994; **33**: 2129–2135.
29. Schönbrunner N, Wey J, Engels J, Georg H, Kiefhaber T. Native-like β-structure in a trifluoroethanol-induced partially folded state of the all-β-sheet protein tendamistat. *J. Mol. Biol.* 1996; **260**: 432–445.
30. Buck M. Trifluoroethanol and colleagues: cosolvents come of age. Recent studies with peptides and proteins. *Q. Rev. Biophys.* 1998; **31**: 297–355.
31. Yang JT, Wu CSC, Martinez HM. Calculation of protein conformation from circular dichroism. *Methods Enzymol.* 1986; **130**: 208–269.
32. Tanford C. Protein denaturation. C. Theoretical models for the mechanism of denaturation. *Adv. Protein Chem.* 1970; **24**: 1–95.
33. Wu JW, Wang ZX. New evidence for the denaturant binding model. *Protein Sci.* 1999; **8**: 2090–2097.
34. Schellman JA. Selective binding and solvent denaturation. *Biopolymers* 1987; **26**: 549–559.
35. Swietnicki W, Petersen R, Gambetti P, Surewicz WK. pH-dependent stability and conformation of the recombinant human prion protein PrP(90-231). *J. Biol. Chem.* 1997; **272**: 27517–27520.
36. Hornemann S, Glockshuber R. A scrapie-like unfolding intermediate of the prion protein domain PrP(121-231) induced by acidic pH. *Proc. Natl. Acad. Sci. U.S.A.* 1998; **95**: 6010–6014.
37. Swietnicki W, Morillas M, Chen SG, Gambetti P, Surewicz WK. Aggregation and fibrillization of the recombinant human prion protein huPrP90-231. *Biochemistry* 2000; **39**: 424–431.
38. Zou W-Q, Cashman NR. Acidic pH and detergents enhance in vitro conversion of human brain PrPC to a PrPSc-like form. *J. Biol. Chem.* 2002; **277**: 43942–43947.
39. Langella E, Improta R, Barone V. Checking the pH-induced conformational transition of prion protein by molecular dynamics simulations: effect of protonation of histidine residues. *Biophys. J.* 2004; **87**: 3623–3632.
40. Borchelt DR, Taraboulos A, Prusiner SB. Evidence for synthesis of scrapie prion proteins in the endocytic pathway. *J. Biol. Chem.* 1992; **267**: 16188–16199.
41. Knaus KJ, Morillas M, Swietnicki W, Malone M, Surewicz WK, Yee VC. Crystal structure of the human prion protein reveals a mechanism for oligomerization. *Nat. Struct. Biol.* 2001; **8**: 770–774.
42. Wopfner F, Weidenhöfer G, Schneider R, von Brunn A, Gilch S, Schwarz TF, Werner T, Schätz HM. Analysis of 27 mammalian and 9 avian PrPs reveals high conservation of flexible regions of the prion protein. *J. Mol. Biol.* 1999; **289**: 1163–1178.

